

UNCLASSIFIED

AD **404 883**

---

DEFENSE DOCUMENTATION CENTER

FOR

SCIENTIFIC AND TECHNICAL INFORMATION

CAMERON STATION, ALEXANDRIA, VIRGINIA



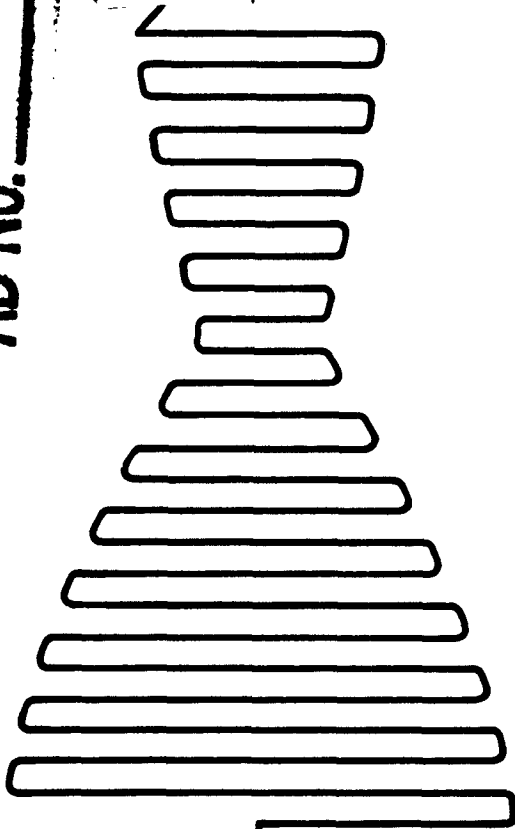
UNCLASSIFIED

NOTICE: When government or other drawings, specifications or other data are used for any purpose other than in connection with a definitely related government procurement operation, the U. S. Government thereby incurs no responsibility, nor any obligation whatsoever; and the fact that the Government may have formulated, furnished, or in any way supplied the said drawings, specifications, or other data is not to be regarded by implication or otherwise as in any manner licensing the holder or any other person or corporation, or conveying any rights or permission to manufacture, use or sell any patented invention that may in any way be related thereto.

CATALOGED BY ASTIA  
AS AD NO. \_\_\_\_\_

404883

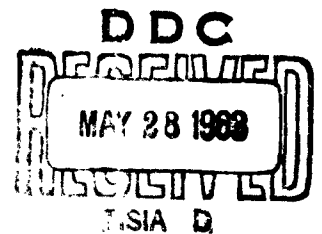
404 883



**ROCKETDYNE**

A DIVISION OF NORTH AMERICAN AVIATION, INC.

CANOGA PARK, CALIFORNIA



6335

R-5179

**FINAL REPORT**  
**RESEARCH IN HYBRID COMBUSTION**  
(1 December 1961 through 31 January 1963)

**ROCKETDYNE**

A DIVISION OF NORTH AMERICAN AVIATION, INC.


6633 CANOGA AVENUE  
CANOGA PARK, CALIFORNIA

Contract No. Nonr 3016(00)  
G.O. 5693

**PREPARED BY**

T. Houser

**APPROVED BY**

  
R. J. Thompson, Jr.  
Director, Research

NO. OF PAGES 45 & v

**REVISIONS**

DATE 15 May 1963

DATE	REV. BY	PAGES AFFECTED	REMARKS

**ROCKETDYNE**  
A DIVISION OF NORTH AMERICAN AVIATION, INC.

---

Reproduction in whole or in part  
is permitted for any purpose of  
the United States Government.

### FOREWORD

This summary report was prepared in compliance with contract number Nonr 3016(00) and covers research accomplished principally during the period 1 December 1961 through 31 January 1963. The personnel associated with the program during this period were Dr. T. Houser, Dr. M. V. Peck, and Dr. H. N. Chu; Dr. S. S. Penner was a consultant.

### ABSTRACT

The instantaneous surface regression rates have been calculated as functions of time and axial distance from the radius vs time data obtained from plexiglas combustion. Temperature measurements of the fuel behind the regressing surface have been made. Additional experiments were carried out to examine the burning rates of different fuels such as polystyrene, polyethylene, 30 and 60 % aluminum, 30 % titanium hydride, and 1/4 and 1/2 % carbon in plexiglass. The significance of the burning rate and temperature measurement results is discussed.

**ROCKETDYNE**  
A DIVISION OF NORTH AMERICAN AVIATION, INC.

---

CONTENTS

Foreword. . . . .	iii
Abstract . . . . .	iii
Introduction and Objectives . . . . .	1
Experimental . . . . .	3
Results . . . . .	5
Time Dependence of Radius and Burning Rates . . . . .	5
Temperature Profile of Fuel Blocks . . . . .	16
Discussion . . . . .	21
Pyrolysis vs Oxidative Degradation . . . . .	21
Combustion Considerations . . . . .	29
Summary and Recommendations . . . . .	39
<u>Appendix A</u> . . . . .	41
References . . . . .	45

ILLUSTRATIONS

1. Diameter After Burning vs Burning Time, Block 3 . . . .	8
2. Diameter After Burning vs Burning Time, Block 3 . . . .	9
3. Instantaneous Regression Rates at Constant Time . . . .	11
4. Instantaneous Regression Rates at Constant Radius . . . .	12
5. Temperature of Fuel Behind the Surface . . . . .	18
6. First Order Rate Constants for PMMA Pyrolysis . . . . .	43
7. Zero Order Rate Constants for PMMA Pyrolysis . . . . .	44

TABLES

1. Constants for Radius vs Time Equation . . . . .	7
2. Instantaneous Linear Burning Rates . . . . .	10
3. Instantaneous Linear Burning Rates at Constant Radius . .	14
4. Instantaneous Mass Burning Rates . . . . .	15
5. Temperature Profiles of Fuel Blocks . . . . .	17
6. Correction of Surface Temperature . . . . .	23
7. Calculated Mass Burning Rates . . . . .	27
8. Ratio of Instantaneous Rates . . . . .	30
9. Time Dependence of Heat Transfer Parameter . . . . .	33
10. Regression Rates at Different Flowrates . . . . .	34
11. Comparison of Surface Regression Rates of Fuels . . . .	36
12. PMMA Pyrolysis Rates . . . . .	42

## INTRODUCTION AND OBJECTIVES

This research program in hybrid combustion has been concerned with the investigation of the processes (both physical and chemical) involved in the interactions between solid polymeric fuels and gaseous oxygen. The objective of these studies has been to determine experimentally which processes are important in affecting the surface regression rates, and to develop a suitable theoretical model to account for the observed results.

A simplified theory of hybrid combustion as sophisticated as the classical treatment of Burke and Schumann (Ref. 1) for the flame shape in cylindrical diffusion flames was presented for the plexiglass-oxygen system (Ref. 2). This theory involved a model obtained using the following assumptions:

1. Chemical reactions are confined to the flame front, considered an infinitely thin mathematical surface close to the wall, to which the fuel and oxidizer are delivered in stoichiometric proportions and are, therefore, consumed instantaneously. For this reason, no fuel exists in the core and no oxygen exists in the annular region between the flame front and the wall.
2. The pressure gradient is negligible and the linear flow velocities are constant. Hence, the axial velocity term is neglected, and only radial transport by diffusion is considered. This has been assumed to be, primarily, concentration diffusion.

**ROCKETDYNE**  
A DIVISION OF NORTH AMERICAN AVIATION, INC.

---

3. Gas mixtures are considered to be binary mixtures composed of the major constituent (either fuel or oxidizer, depending on location beneath or above the flame front) and the rest of the gas mixture as an average.
4. The product of gas density and binary diffusion coefficient is assumed to be independent of radial and axial distances and temperature.
5. No distinction is made between types of flow, and appropriate applicable transport coefficients are to be used for the axisymmetric conditions.
6. The binary diffusion coefficients of fuel and oxygen through nonreacting gas are numerically equal.

With proper definition of the diffusion parameters, this theory may be applied to all types of flow and, in particular, to the turbulent flow conditions examined experimentally.

The purpose of the more recent work has been to define better the contributions of the experimental parameters to the observed regression rates (Ref. 3 through 5) and to determine the validity of the above assumptions. In this reporting period, effort was directed toward obtaining better defined functions of radius with time at the two entrance Reynolds numbers (55,000 and 36,000) and, from these functions, calculating instantaneous regression rates. In addition, the temperature profile in the solid fuel ahead of the regressing surface was further examined, and the isothermal polymer pyrolysis rates and surface regression rates were compared.

### EXPERIMENTAL

The basic apparatus has been described in previous reports (Ref. 2 and 5). The tubular combustor configuration was used for the experimental program. The mixing and flow stabilization tube, which was a 2-inch square duct, has been replaced by a 1-inch diameter tube to reduce the turbulence caused by the abrupt change in diameter at the entrance. In a typical run, a fuel cylindrical surface, composed of 3 by 3 by 2-inch blocks with 1-inch diameter concentric holes aligned with the holes of the facing and backing plates, is burned for the specified time. The weight lost by each block is measured to determine the surface regression; axisymmetric burning is assumed. The axial length (number of blocks), the composition and temperature of fuel, the time of burning, and the initial diameter of the concentric hole may be varied. Thermocouples may be imbedded between adjacent fuel blocks at any desired radial distance to measure the increase in temperature at that position as the burning surface approaches. The latest thermocouples used in this study were chromel-alumel of either 1- or 0.6-mil diameter wire.

The thermogravimetric balance apparatus has been described in Ref. 2. The experimental procedure consisted of observing the weight loss of a block of polymer as a function of time, at a constant temperature, and in the presence of different oxygen-nitrogen mixtures.

## RESULTS

### TIME DEPENDENCE OF RADIUS AND BURNING RATES

To understand the hybrid burning process better, it was believed that instantaneous burning rates at definite axial positions should be examined, since these would be more meaningful than time and length dependent averages. To do this, it was necessary to make runs at several values of  $t$  and then derive an  $r(t)$  equation. This was done with plexiglass (PMMA), as a fuel, primarily at two entrance Reynolds numbers, 55,000 (22.0 gm  $O_2$ /sec) and 36,000 (14.4 gm  $O_2$ /sec), with additional experiments at 6000 (2.4 gm  $O_2$ /sec). On ignition, a line pressure of about 3 or 4 psig was observed at the 55,000 flow which reduced to zero after about 10 to 15 seconds. The lower flowrates exhibited no pressure rise in the line. It is believed that the small pressure rise would have a negligible effect on the burning rate.

By use of the Research Multiple Correlation Computer Program, which applies various statistical tests attempting to obtain the best fit of the supplied functions to the experimental data, Eq. 1 was obtained for radius vs time:

$$r = A + Bt^{0.8} + Ct^{0.3} \quad (1)$$

where

A, B, and C = constants

Table 1 summarizes the data, and Fig. 1 and 2, which present a plot of final radius vs time, illustrate typical fits of data and equation. The same equation was used for all blocks at the higher flowrates and for the entire time range. It must be re-emphasized that Eq. 1 was not intended to have theoretical significance. It was to be used only to determine the time and axial dependences of the regression rates.

The curves presented in Fig. 1 and 2 are not very accurate at times less than 10 seconds, and the slopes go to infinity at  $t = 0$ . A perfect fit would require a sigmoidal curve to indicate the surface heatup time just following ignition. According to the data,  $t$  for inflection of the sigmoid (point of maximum slope) would be below 10 seconds, but accurate data could not be obtained for these short times. Thus, the heatup time was not defined experimentally.

By differentiation of Eq. 1, the regression rate as a function of time can be obtained:

$$\dot{r} = 0.8 B/t^{0.2} + 0.3 C/t^{0.7} \quad (2)$$

The results of these calculations are summarized in Table 2. Figure 3 and 4 illustrate typical examples. It is interesting to note that the regression rates at the 6000 flow are about constant with time and axial distance, although the average rates (over time and distance) decrease somewhat with time, as indicated on the following page.

**ROCKETDYNE**  
A DIVISION OF NORTH AMERICAN AVIATION, INC.

TABLE 1

CONSTANTS FOR RADIUS VS TIME EQUATION

$$r = A + Bt^{0.8} + Ct^{0.3} \text{ (cm)}$$

Oxygen Flow	36,000, 21 Runs				55,000, 22 Runs			
Block/Constants	A	B X100	C X10	$\sigma^*$ X100	A	B X100	C X10	$\sigma^*$ X100
1	0.877	0.183	2.59	1.5	0.940	0.176	2.42	1.2
2	1.040	1.16	1.25	1.2	1.101	1.38	1.03	1.2
3	1.131	1.31	0.783	1.0	1.186	1.61	0.550	1.0
4	1.139	1.24	0.782	1.2	1.160	1.42	0.786	0.9
5	1.086	1.12	1.11	1.5	1.083	1.18	1.27	1.0
6	0.993	0.98	1.53	1.1	0.992	0.933	1.80	1.1
7	0.976	0.98	1.58	1.5	0.987	0.947	1.84	1.5
8	1.000	1.10	1.41	1.5	1.021	1.07	1.70	2.4
9	1.090	1.42	0.896	1.5	1.029	1.16	1.66	1.8
10	1.086	1.39	9.982	1.4	1.015	1.11	1.86	1.7
11	1.120	1.45	0.934	1.2	0.942	0.826	2.42	1.4
12	1.098	1.50	1.13	2.0	0.856	0.811	2.90	2.5

\*Standard deviation of the experimental point from the calculated r vs t curve. These values illustrate the scatter of the data.

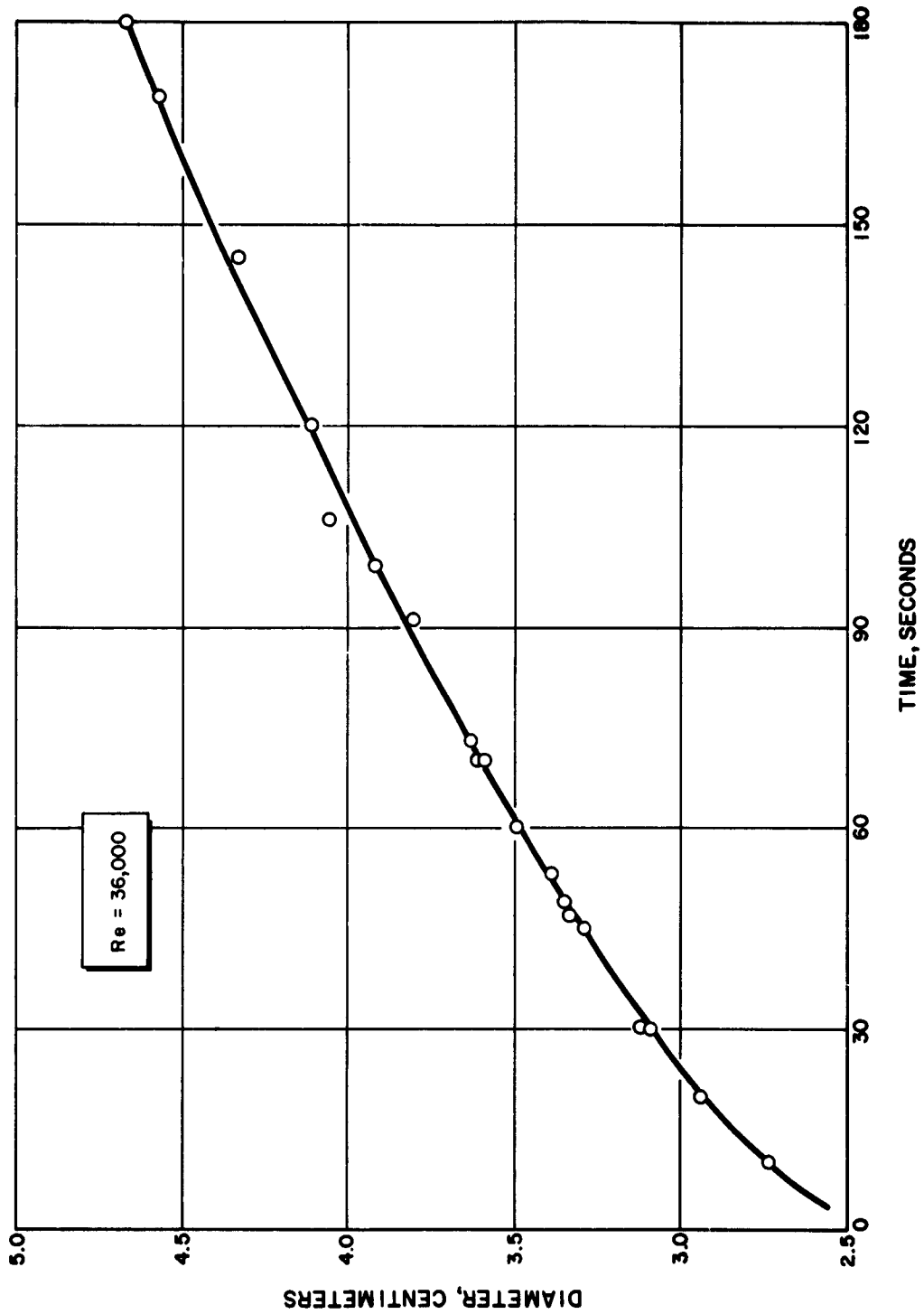


Figure 1. Diameter After Burning vs Burning Time, Block 3

R-5179

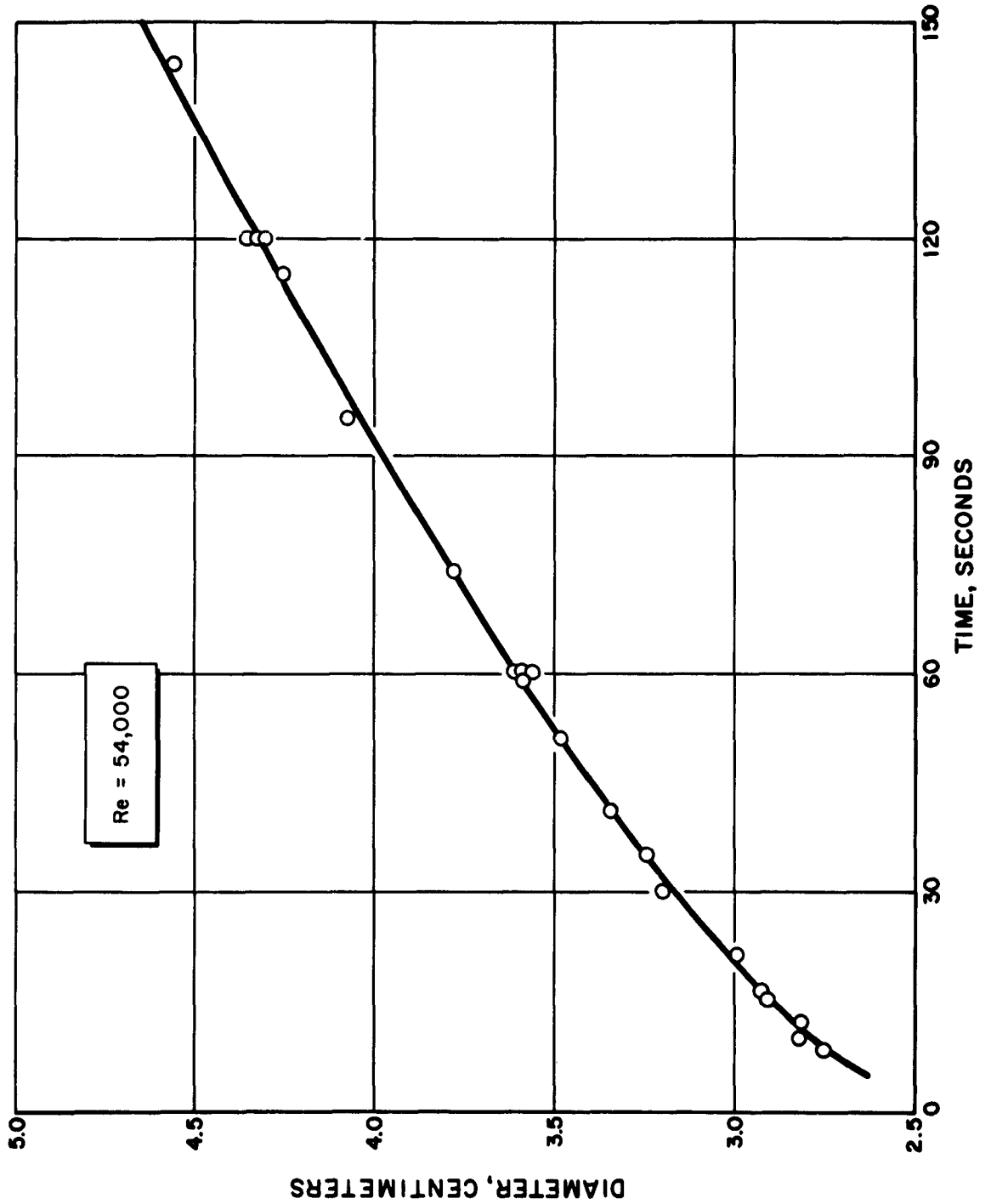


Figure 2. Diameter After Burning vs Burning Time, Block 3

**ROCKETDYNE**  
A DIVISION OF NORTH AMERICAN AVIATION, INC.

TABLE 2

INSTANTANEOUS LINEAR BURNING RATES,  
cm/sec x 10<sup>3</sup>

Time , seconds	Block											
	Flow 55,000, 22 Runs											
	2	3	4	5	6	7	8	9	10	11	12	Average
10	13.1	11.4	11.9	13.6	15.5	15.8	15.6	15.8	16.7	18.7	21.5	—
15	11.1	10.0	10.1	11.2	12.5	12.7	12.6	12.9	13.5	14.8	16.8	12.6
30	8.4	8.0	7.9	8.3	8.8	8.9	9.1	9.3	9.7	10.0	11.3	9.1
45	7.3	7.2	6.9	7.1	7.2	7.4	7.5	7.8	8.0	8.1	9.1	7.6
60	6.6	6.6	6.3	6.3	6.4	6.5	6.7	6.9	7.1	7.0	7.8	6.7
90	5.8	5.9	5.6	5.5	5.3	5.4	5.7	5.9	6.0	-	6.7	5.8
120	5.3	5.5	5.2	5.0	4.8	4.8	5.1	5.3	5.4	-	5.5	5.2
150	5.0	5.2	4.9	4.6	4.4	4.4	4.7	4.9	4.9	-	5.0	4.8
Flow 36,000, 21 Runs												
10	13.3	11.3	10.9	12.3	14.1	14.4	14.0	12.5	12.9	12.9	14.3	—
15	11.0	9.6	9.3	10.2	11.5	11.7	11.5	10.6	10.9	11.0	12.1	10.9
30	8.2	7.5	7.2	7.6	8.2	8.4	8.4	8.2	8.4	8.5	9.2	8.2
45	6.9	6.5	6.2	6.5	6.9	7.0	7.1	7.2	7.2	7.4	8.0	7.0
60	6.2	6.0	5.7	5.8	6.1	6.2	6.3	6.5	6.6	6.7	7.2	6.3
90	5.3	5.3	5.0	5.1	5.2	5.2	5.4	5.8	5.8	5.9	6.3	5.5
120	4.9	4.8	4.6	4.6	4.6	4.7	4.9	5.3	5.3	5.4	5.8	5.0
180	4.3	4.3	4.1	4.0	3.9	4.0	4.2	4.7	4.7	4.8	5.1	4.4
Flow 6000, 4 Runs												
60-180*	3.8	3.6	3.4	3.5	3.4	3.9	3.9	3.9	3.8	3.7	4.4	3.8

\*Constant with time

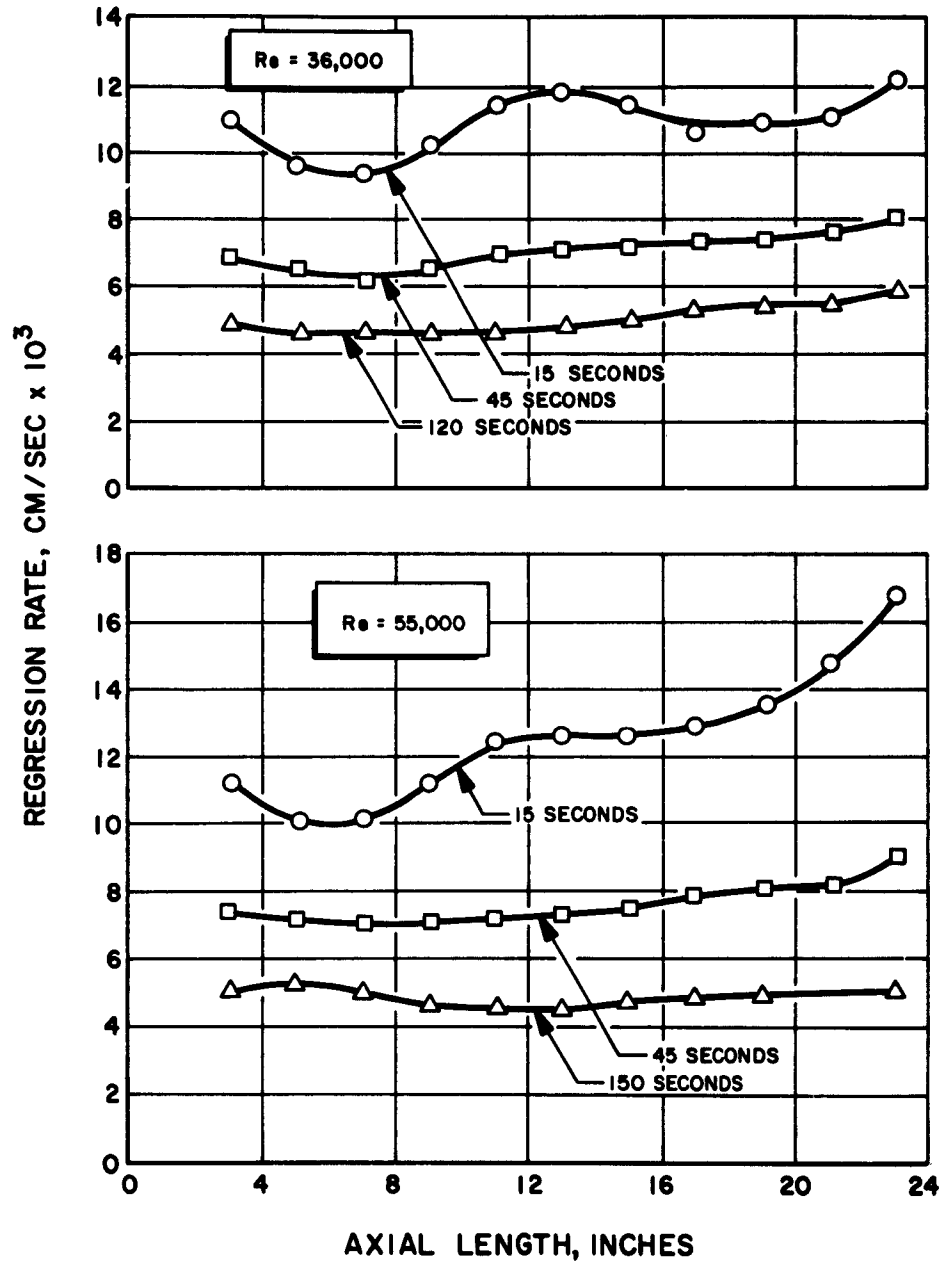


Figure 3. Instantaneous Regression Rates at Constant Time

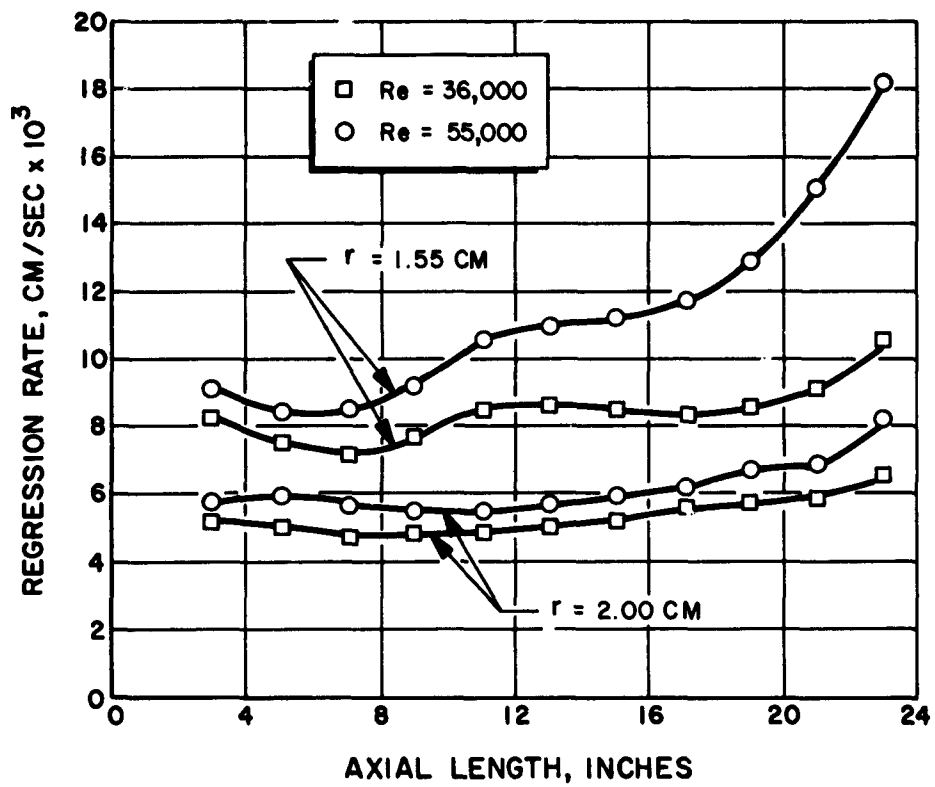


Figure 4. Instantaneous Regression Rates at Constant Radius

**ROCKETDYNE**  
A DIVISION OF NORTH AMERICAN AVIATION, INC.

time	$\dot{r}$ (av)
60	4.2
80	4.0
100	3.9
180	3.9

This variation is due to the changes in rates prior to 60 seconds and is slight, but does illustrate how misconceptions may evolve from averages.

There are two other ways of presenting the data: as linear rates at constant radius (Table 3), and as total mass burning rates (Table 4). The numbers for Table 4 are obtained through the use of Eq. 1, 2 and 3, and are expressed per cm of axial length:

$$\dot{M} = \rho \pi l (r_2^2 - r_1^2) / \Delta t = \rho \pi (r_2 + r_1)(r_2 - r_1) / \Delta t \quad (3)$$

where

$$l = 1 \text{ cm}$$

or

$$M = 2\rho \pi r \dot{r} \text{ (for instantaneous } \dot{r} \text{)*}$$

$\rho$  = density of polymer

It can be seen from Table 4 that the changes in  $\dot{M}$  are very small after 60 seconds.

$$^* \lim_{\Delta t \rightarrow 0} (r_2 - r_1) / \Delta t = \dot{r} \text{ and } (r_2 + r_1) = 2r_{av} = 2r \text{ for small } \Delta r \text{'s.}$$

TABLE 3

INSTANTANEOUS LINEAR BURNING RATES AT CONSTANT RADIUS,

cm/sec X  $10^3$

r, centimeter	Block											
	2	3	4	5	6	7	8	9	10	11	12	
Flow 55,000												
1.55	9.1	8.4	8.5	9.3	10.4	10.8	11.1	11.6	12.9	15.1	18.1	
1.70	7.4	7.1	7.0	7.3	7.8	8.1	8.4	8.8	9.7	10.8	13.1	
2.00	5.8	5.9	5.6	5.5	5.5	5.7	6.0	6.3	6.7	6.9	8.4	
2.30	5.0	5.3	4.9	4.6	4.4	4.5	4.9	5.2	5.4	-	6.2	
Flow 36,000												
1.40	11.8	10.2	10.0	11.4	12.3	12.3	11.9	11.1	11.7	12.8	15.2	
1.55	8.4	7.4	7.1	7.8	8.5	8.6	8.5	8.3	8.6	9.1	10.6	
1.70	6.7	6.2	5.9	6.3	6.7	6.7	6.8	7.0	7.1	7.5	8.5	
2.00	5.2	5.0	4.7	4.8	4.9	5.0	5.2	5.6	5.7	5.9	6.6	
2.30	4.4	4.4	4.1	4.1	4.1	4.1	4.4	4.9	5.0	5.2	5.7	

**ROCKETDYNE**  
A DIVISION OF NORTH AMERICAN AVIATION, INC.

**TABLE 4**

INSTANTANEOUS MASS BURNING RATES,  
gm/sec/cm length x 100

Time, seconds	Block												Total gm/sec l=61cm
	O <sub>2</sub> Flow 55,000, 22.0 gm/sec												
	1	2	3	4	5	6	7	8	9	10	11	12	
10	16.5	13.7	11.9	12.5	14.3	16.3	16.7	16.6	16.9	18.2	20.6	23.8	-
15	13.2	12.0	10.8	11.1	12.3	13.8	14.1	14.2	14.5	15.5	17.2	19.9	8.7
30	9.1	10.1	9.5	9.5	10.0	10.7	11.0	11.2	11.6	12.3	13.1	15.1	6.8
45	7.4	9.4	9.1	8.9	9.1	9.5	9.7	10.0	10.5	11.0	11.4	13.1	6.0
60	6.4	9.0	8.9	8.6	8.7	8.8	9.0	9.4	9.9	10.3	10.5	12.0	5.7
90	5.3	8.7	8.8	8.3	8.2	8.1	8.3	8.8	9.2	9.6	-	10.8	5.2
120	4.7	8.6	8.9	8.3	8.0	7.7	8.0	8.5	9.0	9.3	-	10.1	5.1
150	4.3	8.7	9.1	8.4	7.9	7.5	7.7	8.3	8.8	9.1	-	9.7	4.9
O <sub>2</sub> Flow 36,000, 14.5 gm/sec													
10	17.3	13.6	11.6	11.2	12.7	14.3	14.5	14.1	12.7	13.2	13.5	15.2	-
15	13.8	11.7	10.2	9.9	11.0	12.2	12.4	12.1	11.3	11.6	11.9	13.4	7.2
30	9.6	9.5	8.7	8.3	8.9	9.6	9.8	9.8	9.6	9.8	10.1	11.3	5.9
45	7.9	8.7	8.1	7.7	8.1	8.6	8.7	8.8	9.0	9.1	9.5	10.5	5.3
60	6.8	8.2	7.8	7.4	7.7	8.1	8.2	8.3	8.7	8.8	9.1	10.2	5.1
90	5.7	7.8	7.5	7.1	7.3	7.5	7.6	7.8	8.4	8.3	8.9	9.9	4.8
120	5.0	7.6	7.5	7.1	7.1	7.2	7.3	7.6	8.4	8.5	8.9	9.8	4.7
180	4.2	7.6	7.6	7.1	7.0	7.0	7.1	7.5	8.6	8.6	9.0	9.9	4.6

**ROCKETDYNE**  
A DIVISION OF NORTH AMERICAN AVIATION, INC.

---

An attempt to run the combustor at higher pressures (about 50 psig) was not successful because of vibration and chatter of the apparatus. These runs were discontinued because of safety factors and of considerable doubt as to the significance of the data obtainable under these conditions. Modifications of the apparatus would be necessary before pressurized runs could be made.

**TEMPERATURE PROFILE OF FUEL BLOCKS**

It was found that the temperature profile of the fuel blocks behind the regressing surface followed Eq. 4.

$$T = T_s \exp (-bX) \quad (4)$$

where

$T$  = temperature above initial block temperature at  $X$  centimeters from the surface

$T_s$  = surface temperature above initial block temperature

The derivation of this equation is discussed in a following section. Table 5 summarizes the results of thermocouple measurements and Fig. 5 indicates a typical fit of data and equation. These values are considerably higher than those previously reported (Ref. 5). The reason for the difference is that 0.6- to 1-mil thermocouples were used in the later experiments, whereas previously 10-mil wire was used. Heat losses along wires as small as 1 mil are believed to be negligible.

**ROCKETDYNE**  
A DIVISION OF NORTH AMERICAN AVIATION, INC.

**TABLE 5**

**TEMPERATURE PROFILES OF FUEL BLOCKS**

$$T = T_s \exp (-bX)$$

$T_s$ , C°	$b$ , cm <sup>-1</sup>	Material
36,000		
365	9.03	PMMA
330	8.88	PMMA
310	11.39	PMMA
325	11.00	PMMA
315	12.20	PMMA
360	11.03	PMMA + 1/4 % C
360	9.30	PMMA + 1/4 % C
6000*		
350	6.53	PMMA
370	6.90	PMMA
Average 345 ± 20		

\*The temperature profiles were linear for the first 40 and 35 seconds, respectively, before becoming exponential.

**ROCKETDYNE**  
A DIVISION OF NORTH AMERICAN AVIATION, INC

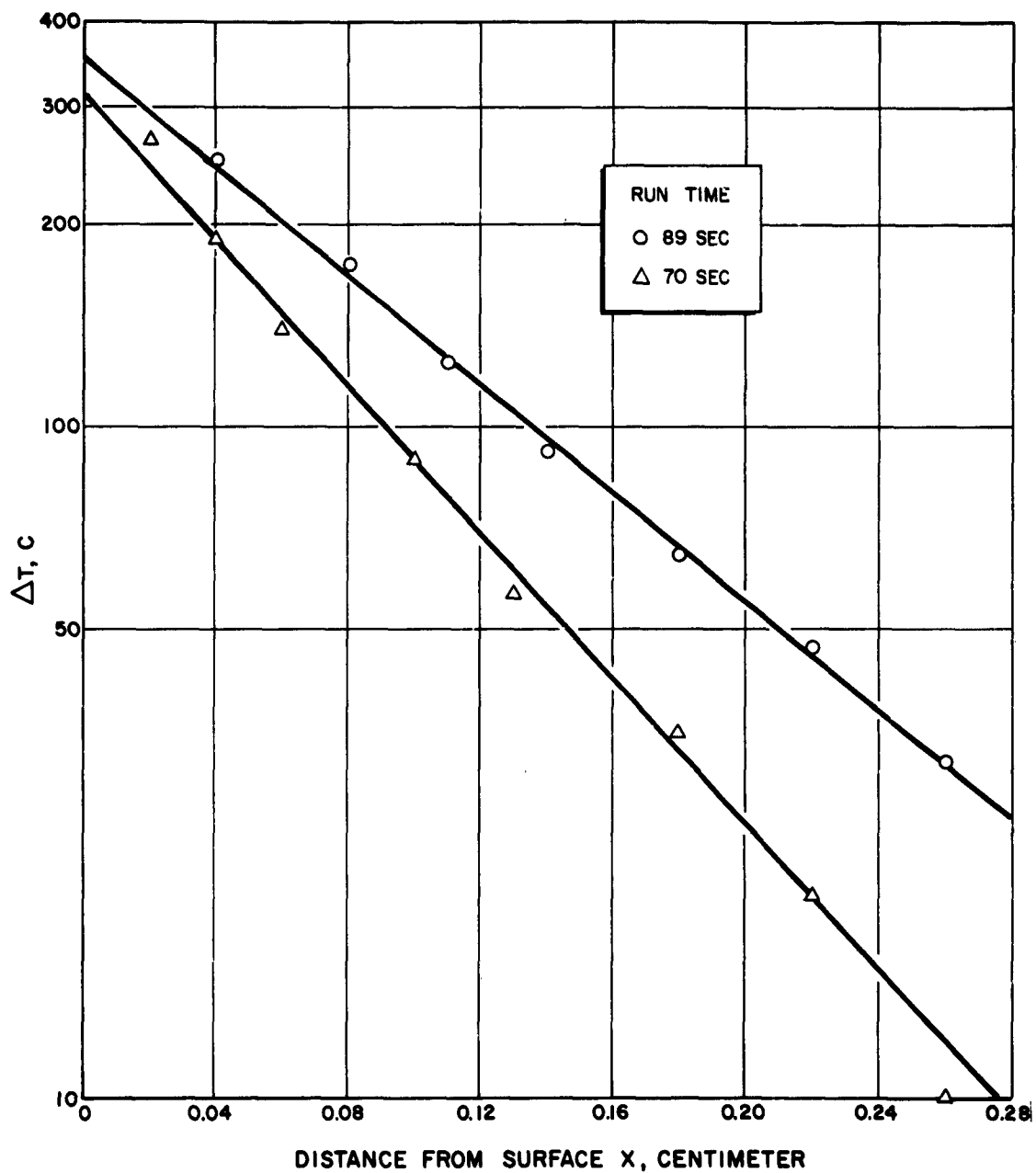


Figure 5. Temperature of Fuel Behind the Surface

Two important observations should be noted. First, the surface temperatures are the same (within experimental deviation) for opaque (carbonized) and clear blocks. Thus, radiation does not appear to influence these temperature readings. Secondly, the temperature profiles obtained with the lower flowrate (6000) were almost linear for about the first half of the run time. After this initial period, they followed the exponential form. The initial temperature rise registered by the thermocouple was more rapid for the 6000 flowrate runs. This was probably due to smaller burning rates, and, thus, less heat was used up in pyrolysis.

It is apparent that small changes in surface temperatures cannot be detected by this technique because of the relatively large scatter. The deviations are probably due to uncertainties in the exact position of the thermocouple with respect to the surface.

Attempts were made to obtain optical pyrometer measurements of the flame through the PMMA walls. It was considered that, although the absolute value of the temperatures would be inaccurate, trends with time and axial distance may be meaningful. The values ranged from 1080 to 1340 K, but too much scatter was obtained for interpretation.

## DISCUSSION

Discussion of the experimental results has been divided into two sections. The first is concerned with the surface temperature measurements and the isothermal pyrolysis rate data that are available. The second is concerned with the burning rate data obtained in the combustor, and comparison of these data with the presently accepted theory. These sections also contain tabulations and discussions of data considered only in a qualitative manner in previous progress reports.

### PYROLYSIS VS OXIDATIVE DEGRADATION

#### Temperature Measurements

Derivation of the Heat Conduction Equation. Equation 4 was obtained from Eq. 5, which is the differential equation for a moving boundary cylindrical surface heat conduction problem for a semi-infinite solid:

$$dT/dt = kd^2T/dX^2 + [(k/a) + \dot{r}] dT/dX = 0 \quad (5)$$

or

$$d^2T/dX^2 = -b dT/dX$$

where

$k$  = thermal diffusivity of the fuel, sq cm/sec

$X$  = linear distance of the thermocouple from the surface

$a$  = distance from center of hole to thermocouple, a  
constant ( $R + X$ )

$T$  = temperature at  $X$ , referenced to initial temperature of block

$T_s$  = extrapolated surface temperature, referenced to initial temperature of block

$b = (1/a + \dot{r}/k)$

$\dot{r}$  = average regression rate

To arrive at Eq. 4, it was necessary to assume that temperatures and regression rates were independent of time (steady state and constant coefficients). The good fit of the data to the simple exponential form indicates that these assumptions were justified (Fig. 5).

The average value for  $T_s$  is  $345 \pm 20$  (average derivation) above initial temperature (25 C), 370 C. A difference of  $10^{-2}$  centimeters in  $X$  would change the extrapolated  $T_s$  value about 30 degrees; therefore, the uncertainty in  $X$  can easily account for the deviations observed.

Correction of the Extrapolated  $T_s$ . Because of the endothermicity of the polymer degradation, the extrapolated surface temperature, as obtained from Eq. 4 is low. The heat absorbed during reaction gives a more rapid drop in temperature with distance than would be predicted from simple heat conduction theory. The thickness of the reacting layer is  $X_r$ , at which distance the temperature has dropped to  $T_r$ . The temperatures at all values of  $X$  greater than  $X_r$  will then follow Eq. 4. If it is assumed that the pyrolysis rate at  $T_r$  is about 100 times slower than the rate at  $T_a$ , the actual surface temperature, then  $T_a$  can be calculated for each  $X_r$  using Eq. 6 obtained from chemical kinetics:

$$\frac{K_{T_a}}{K_{T_r}} = 100 = \exp \left[ -E/R(1/T_a - 1/T_r) \right] \quad (6)$$

where

$K$  = rate constants

$E$  = activation energy = 33,000 (Ref. 6)

$T_a$  and  $T_r$  are in degrees K

$R$  = the gas constant = 1.99

The  $T_r$ 's are obtained from Eq. 4 for each  $X_r$ . The results of these calculations are shown in Table 6, using approximately the average experimental values in Eq. 4 and  $T_g = 360$  C.

TABLE 6

CORRECTION OF SURFACE TEMPERATURE  
(360 C)

$X_r \times 100$ centimeters	$T_r$ , C	$T_a$ , C	Correction, C
3.5	260	360	0
3.0	275	375	15
2.0	300	410	50
1.0	330	450	90
0.5	345	475	115
0.1	355	490	130

The largest value of 0.035 centimeter for  $X_r$  represents the conduction profile, since  $T_a = T_g = 360$  C, which would be obtained only if a negligible fraction of the heat was absorbed for pyrolysis, i.e., heat conduction > rate of heat absorbed. Thus, it is the maximum value possible for an endothermic pyrolysis. The smallest value tabulated,  $10^{-3}$  centimeters, is the minimum value to be examined because the correction will not change significantly for smaller distances.

Comparison of Isothermal Pyrolysis Rates to  
Regression Rates

The next step is to compare the rate of pyrolysis at the corrected temperature,  $T_a$ , as predicted from isothermal pyrolysis rate data, to the observed regression rates and temperatures. Presented below is a tabulation of the PMMA pyrolysis rate constants measured in vacuum by Madorsky (Ref. 6), which followed Eq. 7.

$$K = 3.2 \times 10^9 \exp (-16,500/T) (\text{min}^{-1}) \quad (7)$$

Temperature, C	$K \times 10^3,$ $\text{min}^{-1}$
240	1.9
250	3.7
260	6.9
270	11.0

These values were obtained by extrapolating the rate data to 0% decomposed, and represent the upper limit of the data.

On re-examination of the pyrolysis rate data obtained at Rocketdyne, it was found that some values reported (Fig. 11, Ref. 2) were in error. The corrected values are presented and discussed in Appendix A. There is general agreement between the data obtained by Madorsky (Ref. 6) and that obtained in this laboratory.

It is now necessary to take the corrected  $T_g$ , or  $T_a$ , and the rate parameters from Eq. 7 and calculate the theoretical mass burning rates. First, a rate equation to be used in a system with an exponential temperature gradient must be developed. The development is presented below.

For a first order reaction, such as PMMA pyrolysis (Ref. 6), the mass pyrolysis rate is proportional to the mass heated and the rate constant, Eq. 8.

$$\dot{M} = Mf \exp (-E/RT) \quad (8)$$

where

$\dot{M}$  = mass pyrolysis rate

$M$  = mass heated to temperature,  $T$ , which is in degrees K

$f$  = pre-exponential factor

$E$  = activation energy

$R$  = gas constant

If the mass pyrolysis rate per unit area,  $\dot{m}$ , is considered,  $M$  can be replaced by  $\rho V/A$  (density times volume divided by surface area), which results in  $\rho X$  (where  $X$  is the distance from the surface). Thus, Eq. 9 can be written:

$$\dot{m} = \rho Xf \exp (-E/RT) \quad (9)$$

Since the temperature is a function of  $X$ , the total  $\dot{m}$  is the sum of the rates over the entire range of temperatures; thus, Eq. 10 results:

$$\dot{m} = \rho f \int_0^s \exp(-E/RT) dX \quad (10)$$

where

$s$  = thickness of the polymer.

The temperature dependence on  $X$  as expressed by Eq. 11 can be substituted for  $T$ :

$$T' = T_a' \exp(-cX) \quad (11)$$

Temperatures ( $T'$ ) must be in K, and can be calculated from the values for  $X_r$ ,  $T_r$ , and  $T_a$  in Table 6. The difference between Eq. 4 and 11 is the temperature scale and the exponential coefficients in the latter pyrolysis is considered. Equation 11 is a simple exponential which approximates satisfactorily Eq. 4 for small values of  $X$ , which is the region of importance for the pyrolysis. If a new variable,  $y$ , is defined by Eq. 12:

$$y = E/RT = (E/RT_a) \exp(cX) \quad (12)$$

$$\text{and} \quad dy = (cE/RT_a) \exp(cX) dX$$

$$\text{or} \quad dX = dy/cy$$

then Eq. 10 through 12 can be combined to give Eq. 13:

$$\dot{m} = \rho f/c \int_{E/RT_a}^{\infty} \exp(-y)/y dy \quad (13)$$

**ROCKETDYNE**  
A DIVISION OF NORTH AMERICAN AVIATION, INC.

The upper limit of  $\infty$  can be used in place of  $s$ , since the value of the integral is not changed significantly at values of  $X$  larger than  $X_r$  because of the rapid decrease in temperature (the error introduced by using  $\infty$  is about 1 percent). The value of this integral has been evaluated by a series solution. The results of the calculated and observed burning rates are presented in Table 7.

TABLE 7

CALCULATED MASS BURNING RATES

$T_r$ , K	$T_a$ , K	$X_r \times 100$ , centimeters	$c$	$\int_0^\infty \frac{x}{E/RT_a} \times 10^{13}$	$\rho f/c \times 10^8$	$\dot{m} \times 10^4$ , gm/sec/sq cm
533	633	3.5	4.9	1.8	7.8	1.4
548	648	3.0	5.6	3.3	6.8	2.2
573	683	2.0	8.7	12.8	4.4	5.7
603	723	1.0	18.1	52	2.1	10.9
618	748	0.5	38.2	115	1.00	11.5
628	763	0.1	195	180	0.20	3.6

Experimental\*  $\dot{m} = 100 \times 10^{-4}$  gm/sec/sq cm

\*This value represents an average number over about 10 runs of 60 second duration, 24-inch axial length, and 36,000 flow.

It can be seen that the predicted  $\dot{m}_g$  are too low by a factor of about 10, even using the highest rates calculated from the highest isothermal rates.

Some explanations that can be advanced at this time for the low calculated values are:

1. The polymer regression rate is not governed solely by pyrolysis; oxidative degradation contributes. This may be caused by  $O_2$ ,  $CO_2$ ,  $CO$ ,  $H_2O$  or various radical intermediates initiating chain degradations.
2. Some fuel is blown off the surface as the polymer softens. This appears unlikely for PMMA but may be significant in the higher rates observed for polystyrene (PS) since it softens at lower temperatures.
3. The temperature measurements are significantly low due to heat losses. An approximate calculation shows that if the temperature correction is in error by 80 K and the  $X_r$  is about 0.02 cm, the calculated  $\dot{m}$  is still too low by a factor of 2 ( $\dot{m} = 49 \times 10^{-4}$ ).
4. The extrapolation of the isothermal rate data may be in error and the rates are much faster than Eq. 7 predicts.

It is believed that the above calculation reveals a serious discrepancy and that elucidation of these differences may lead to a much better understanding of hybrid combustion. The ability of oxygen to increase the rate of depolymerization of PMMA by as much as a factor of 10 is shown by the results tabulated in the Appendix Table 1.

## COMBUSTION CONSIDERATIONS

The combustion rate data which were obtained during the course of the program are discussed in this section. Most of the experiments were conducted under oxidizer-rich conditions. For PMMA to burn to CO or CO<sub>2</sub> and water, it is necessary to have mixture ratios ( $W_o/W_f$ ) of about 1.1 and 1.9, respectively; as can be seen from Table 9 and 10, the ratio employed experimentally is usually greater.

### Instantaneous Burning Rate Behavior

Table 2, 3, 4, and 8 summarize the instantaneous burning rate behavior. The calculations of slopes ( $r$  vs  $t$ ) at the extreme times (10 and 150 or 180 seconds) are not too reliable because of a lack of data beyond these points.

General trends can be detected. A slight minimum occurs for the two higher flowrates and appears to shift to longer axial distances at larger radii for the 55,000 flow, Table 3. This minimum is probably still caused by an entrance effect since it is much less pronounced with the smoother entrance section. Block 1 is not tabulated in most cases since its behavior is anomalous because of the pronounced entrance effect.

The linear regression rates decrease with time, as predicted, because of the larger port area. The rate appears to show an increase with downstream distance. At the smaller radii the ratio of the instantaneous regression rates for Re 55,000/36,000 increases with axial distance as presented in the previous quarterly report (Ref. 5); but this does not hold at larger radii (Table 8). The fact that the ratio of rates remains

TABLE 8  
RATIO OF INSTANTANEOUS RATES  
(Re 55,000/36,000)

r, centimeters	Block										
	2	3	4	5	6	7	8	9	10	11	12
1.55	1.08	1.13	1.19	1.19	1.22	1.26	1.30	1.40	1.50	1.66	1.71
1.70	1.10	1.14	1.19	1.16	1.16	1.21	1.24	1.26	1.37	1.44	1.54
2.00	1.11	1.18	1.19	1.15	1.12	1.14	1.15	1.13	1.18	1.17	1.27
2.30	1.14	1.23	1.20	1.12	1.07	1.10	1.11	1.06	1.08	-	1.09

constant or drops slightly with axial distance, as is the case for larger radii, would be predicted from flow velocity considerations, because the ratio of velocities also drops slightly. However, the rise observed at smaller radii cannot be explained from flow considerations alone. Similarly, the plateaus and drops evidenced at the shorter times or smaller radii (Fig. 3 and 4), appear real and would require reversal of trends in terms of flow considerations. Other factors must be important.

Another interesting result is that the total mass burning rate,  $\dot{M}$ , is relatively constant with time after about 60 seconds. This is of considerable importance in hybrid grain design. In the following section the accepted regression rate equation, which has been the basis of grain designs is compared to the data obtained in this program.

#### Theory vs Experiment

The accepted equation for the average burning rate as derived by UTC (Ref. 7) and used by Lockheed (Ref. 8) for grain design problems is:

$$\dot{r} = a(\dot{w}_t)^{0.8}/(L)^{0.2} (A)^{0.8} + b \quad (14)$$

**ROCKETDYNE**  
A DIVISION OF NORTH AMERICAN AVIATION, INC.

---

where

$a$  and  $b'$  = complex parameters involved in heat transfer  
(not constants)

$\dot{w}_t$  = total flowrate of propellants

$L$  = grain length

$A$  = port area

The  $b'$  term is the contribution of radiation. It is usually neglected because it is small and difficult to evaluate. As indicated by the present study, radiation effects on rate do not appear important (Table 11). Thus, the  $b'$  term has been neglected in the present calculations.

Table 9 and 10 summarize the data (average  $\bar{r}$ ) for runs employing blocks of 24 inches total length, at various times and flowrates. Equation 14 was used to calculate the parameter  $\underline{a}$ ; the values listed indicate the variation of  $\underline{a}$  with time and oxygen flowrate. Involved in this parameter are ratios of velocities and Stanton numbers, enthalpies of gas and solid phases, viscosities, etc. In view of the complexity of  $\underline{a}$ , these values appear remarkably constant under the range of conditions considered in this program. Two comments are warranted at this time: (1) the function expressed by Eq. 14 ( $\underline{a}$  = approximately constant) appears satisfactory for most applications, although the influence of possible deviations of  $\underline{a}$  with time, flowrates, and especially with different propellant systems should be checked for their effect on grain design, etc.

**ROCKETDYNE**  
A DIVISION OF NORTH AMERICAN AVIATION, INC.

TABLE 9

TIME DEPENDENCE OF HEAT TRANSFER PARAMETER

Time, seconds	$\dot{r}_{av} \times 100,$ gm/sec	Total Propellant Flow, $\dot{w}_t,$ gm/sec	Port Area, A, sq cm	a $\times 1000$
36,000 = 14.4 gm/sec of $O_2$				
15	10.9	21.7	6.60	1.84
30	8.2	20.4	7.95	1.67
45	7.0	19.8	9.07	1.62
60	6.3	19.6	10.3	1.67
90	5.5	19.3	12.5	1.71
120	5.0	19.2	14.7	1.76
180	4.4	19.1	19.0	1.93
55,000 = 22.0 gm/sec of $O_2$				
15	12.6	30.7	7.16	1.71
30	9.1	28.8	8.70	1.54
45	7.6	28.0	10.1	1.45
60	6.7	27.7	11.4	1.45
90	5.8	27.3	13.6	1.45
120	5.2	27.1	15.9	1.49
150	4.8	27.0	18.3	1.54

TABLE 10

REGRESSION RATES AT DIFFERENT FLOWRATES

$Re \times 10^{-3}$ , entrance	$O_2$ Flow, gm/sec	Total Fuel Flow, gm/sec	$\dot{w}_t$ , gm/sec	Port Area A, sq cm	$\dot{r} \times 1000$ , cm/sec	$a \times 1000$
Smooth Entrance *						
6	2.4	2.7	5.1	6.11	4.2	2.15
25	10.0	5.0	15.0	6.98	7.3	1.71
36	14.4	6.3	20.7	7.43	8.9	1.71
55	22.0	7.3	29.3	7.80	10.1	1.54
2 Inch Duct Entrance *						
6	2.4	2.5	4.9	6.07	4.0	2.15
8	3.2	2.9	6.1	6.20	4.5	1.97
37	14.8	6.2	21.0	7.40	8.8	1.67
56	22.4	8.1	30.5	8.07	11.1	1.67
75	30.0	9.8	39.8	8.65	13.0	1.67
Small Hole **						
12	2.4	3.0	5.4	2.60	7.5	1.95
29	5.8	6.0	11.8	3.29	12.9	2.14
61	12.2	9.4	21.6	4.25	17.6	2.23
110	22.0	11.3	33.3	4.80	20.0	2.14

\*Average rate of a 60-second run of 24-inch axial length, initial ID of 1 inch.

\*\*Initial ID of 1/2 inch.

(2) It is believed that experimental values of the parameters making up a are not sufficiently well known, under the conditions of hybrid combustion, to state that theory and experiment are in agreement (or disagreement). The apparent agreement may arise from lack of sensitivity of the rate to the parameters involved or from compensating deviations.

Thus, it appears that too little is known at this time for a rigorous combustion model to be developed; the need for more basic information concerning both chemical and physical processes is still indicated.

#### Regression Rates of Different Fuels

Although the regression rate results, employing different fuels, have been discussed in previous reports (Ref. 3 and 4), Table 11 presents a more complete summary of quantitative values.

Certain points can be mentioned briefly. Preheating or precooling of the fuel blocks had little effect on the rates. The addition of carbon to PMMA appeared to yield a small increase in rate. However, the 10% change observed is probably due to the difference in degree of polymerization of the fuel in the presence of carbon, rather than to an increase in heat transfer from radiation, because PMMA blocks containing more carbon than 1/2% did not cure completely. The small increase in rate from PMMA to 30% Al in PMMA is surprising since several factors would appear to promote a higher rate, for example: The higher flame temperature of an aluminized system, the smaller amount of polymer to pyrolyze per centimeter of distance (the aluminum would be assumed to melt but not vaporize between the wall and the flame), and the higher absorptivity of the opaque wall. The 60% Al and 30% TiH<sub>4</sub> fuels do show a large increase in rate. Again the contribution of the additive to the degree of polymerization of the PMMA is unknown, which may account, at least in part, for differences in rates.

**ROCKETDYNE**  
A DIVISION OF NORTH AMERICAN AVIATION, INC.

TABLE 11

COMPARISON OF SURFACE REGRESSION RATES  
OF FUELS

Fuel	$\dot{r} \times 1000^*$ cm/sec		Initial Fuel Temperature, C
	O <sub>2</sub> Flow 55,000	6000	
PMMA	11.3	4.2	Ambient
PMMA + 30 % Al	12.0	4.7	Ambient
PMMA + 60 % Al	14.8	7.8	Ambient
PMMA + 30 % TiH <sub>4</sub>	14.8	5.0	Ambient
PE	11.4	4.8	Ambient
PS	25.0	9.8	Ambient
PMMA	11.3	-	-20
PMMA	12.1	-	100

	$\dot{r} \times 1000^{**}$ cm/sec			Run Time, seconds
	Fuel, PMMA	PMMA + 1/4 % C	PMMA + 1/2 % C	
O <sub>2</sub> Flow	10.1	11.2	-	30
36,000	8.8	9.5	-	53
	8.5	9.2	-	60
	7.6	8.0	8.3	90
	9.2	-	10.1	45

\*Average rates over two 60-second runs of 24-inch axial length; older 24-inch entrance duct used.

\*\*Average rates, fuels all at ambient temperature; newer 1-inch entrance section used.

The behavior of polyethylene (PE) was similar to PMMA except for a significant amount of melting and liquid ejection. The burning of polystyrene (PS) was considerably different from that of the other fuels. As discussed in previous reports (Ref. 3 and 4) the rate became more rapid immediately following the entrance, and maintained a very high rate of regression which started dropping after about 24 inches (55,000 oxygen flowrate).

A comparison of the pyrolysis rates of PMMA and PS (Ref. 6) indicates that the PS rate is slower in the temperature range studied, contrary to regression rate results. An important contributor to the observed higher rate may be the lower softening and melting points of PS. The roughness of the surface after burning may be indicative of the importance of this factor. In addition, the flame temperature of the PS oxygen system is higher, and, also, if the monomer pyrolyzes at or near the surface, additional heat will be liberated to increase the volatilization rate because styrene has a positive heat of formation.

These results point to a need for a better understanding of relative pyrolysis and oxidative pyrolysis rates, and the influence of additives (metals, etc., on these rates). In addition, the pyrolysis rates of the monomers (e.g., styrene and MMA) must be known better to evaluate their contribution to surface regression rates.

### SUMMARY AND RECOMMENDATIONS

The burning of a solid fuel and a gaseous oxidizer has been studied using primarily plexiglass (PMMA) as the fuel, and oxygen, at various flowrates, as the oxidizer. The burning rates were determined at different values of axial distance and time to define experimentally the rates as functions of these parameters. Additional measurements were made of the temperature of the fuel behind the regressing surface to determine the surface temperature.

The extrapolated surface temperatures appear to be too low to account for the observed regression rates by only a pyrolysis mechanism if the isothermal pyrolysis rates of PMMA are extrapolated to the surface temperature. One or more of the following factors may contribute to the observed difference: (1) oxygen, radical intermediates, or products may accelerate pyrolysis, (2) the temperature measurements may be in error, and (3) the extrapolated pyrolysis rates may be in error. The reason for this difference must be clarified. If (1) is important then extrapolation of behavior to different propellant systems will be extremely difficult unless the interactions and relative reaction rates are known.

Similarly, the high regression rates of polystyrene (PS), greater than two times that of PMMA, can be explained only in part by the difference in flame temperature. The heat of depolymerization plus vaporization of the monomer of PS and PMMA are about 263 and 208 cal/gm, respectively. Thus, the heat transfer rate necessary for the PS burning rate would be almost three times that required for PMMA, which appears unlikely. It

**ROCKETDYNE**  
A DIVISION OF NORTH AMERICAN AVIATION, INC.

---

is possible that the pyrolysis of styrene monomer could account for additional heat since its heat of formation is about (+) 35 kcal/mole (endothermic), but the pyrolysis must occur sufficiently close to or on the surface (thus rapidly) to yield the desired effect. Again, the role of chemical kinetics must be explored further because heat transfer and thermochemistry apparently do not account for the observed results under the conditions of this program.

In conclusion, the heat transfer considerations used to explain regression rate behavior are important. There are indications, however, that chemical kinetics may also contribute significantly to burning rates for hybrids, and that these contributions appear more pronounced in the comparisons between different propellant combinations.

APPENDIX A

This appendix presents tabulations of the rate constants determined for PMMA pyrolysis.

On thorough re-examination of the data reported previously (Ref. 2 Fig. 11 ) it was found that values of two points were in error in the original cursory calculations; the corrected results are presented in Table 12 . It is believed that the results agree fairly well (within a factor of two) with those reported by NBS (Ref. 6 ) (using their average rates rather than those obtained by extrapolating to 0 % decomposed), considering the large difference in size of the polymer samples (a factor of about 250).

The results in Table 12 are the average rates over their entire range of pyrolysis, which appear to be the best representation of the data. No consistent trends with percent volatilized were noted in these data.

Figure 6 and 7 illustrate Arrhenious plots of the data as first- and zero-order pyrolyses reactions, respectively. It appears, within the limitations of the accuracy of the experiments, that the data can be represented almost equally well by either order.

It is believed that the rates reported at the higher temperatures (Ref. 2 ) gave nonlinear Arrhenious plots because of the limitations of the experimental techniques used, rather than because of changes in chemical mechanism. For this reason, they have not been used in the present report. This does not imply that changes in mechanism do not take place at higher temperatures but, rather, that the higher rates measured by the techniques used in this program cannot be interpreted.

**ROCKETDYNE**  
A DIVISION OF NORTH AMERICAN AVIATION, INC.

TABLE 12

PMMA PYROLYSIS RATES

Gas	Temperature, C	$10^3/T$	Initial Weight, grams	Average Rate ( $k_0$ ), mg/min	$k_1 \times 10^3$ $\text{min}^{-1}$
N <sub>2</sub>	256	1.89	1.33	1.5	1.3
N <sub>2</sub>	269	1.84	1.57	2.0	1.4
N <sub>2</sub>	318	1.69	1.42	5.4	4.1
2 % O <sub>2</sub>	230	1.99	1.37	2.0	1.6
2 % O <sub>2</sub>	242	1.94	1.48	3.4	2.5
2 % O <sub>2</sub>	263	1.87	1.55	4.6	3.5
2 % O <sub>2</sub>	281	1.80	1.52	6.0	4.7
2 % O <sub>2</sub>	312	1.71	1.58	11.3	10.8
35 % O <sub>2</sub>	210	2.07	1.58	1.1	0.8
35 % O <sub>2</sub>	225	2.00	1.67	3.2	2.0
35 % O <sub>2</sub>	235	1.97	1.44	3.4	2.6
35 % O <sub>2</sub>	249	1.92	1.22	6.0	5.5
35 % O <sub>2</sub>	262	1.87	1.82	12.3	8.7
100 % O <sub>2</sub>	203	2.11	1.27	0.9	0.7
100 % O <sub>2</sub>	235	1.97	1.56	5.1	3.6
100 % O <sub>2</sub>	247	1.92	1.66	5.7	4.1
100 % O <sub>2</sub>	263	1.87	1.69	10.0	7.0

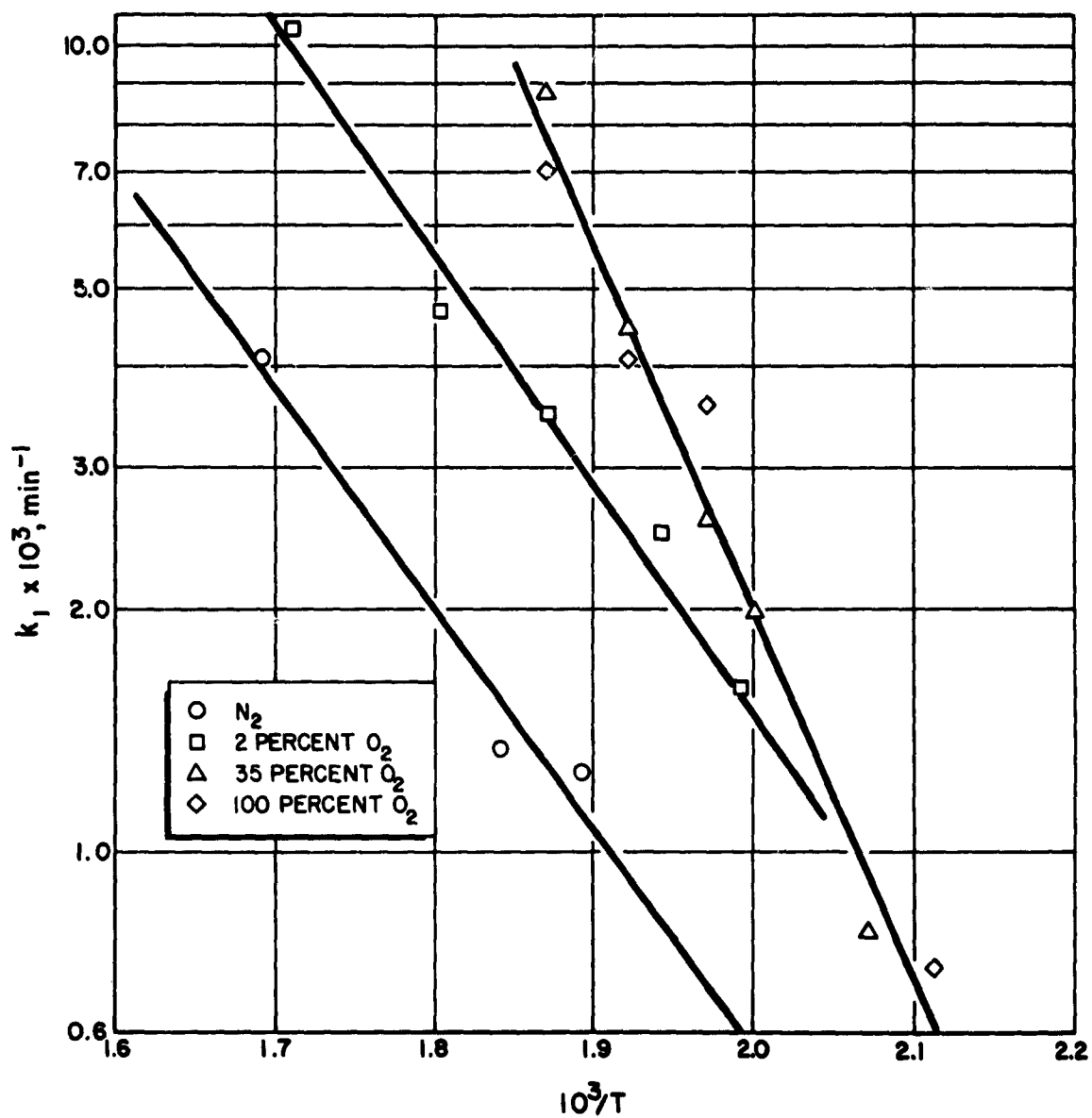


Figure 6. First-Order Rate Constants for PMMA Pyrolysis

**ROCKETDYNE**  
A DIVISION OF NORTH AMERICAN AVIATION, INC

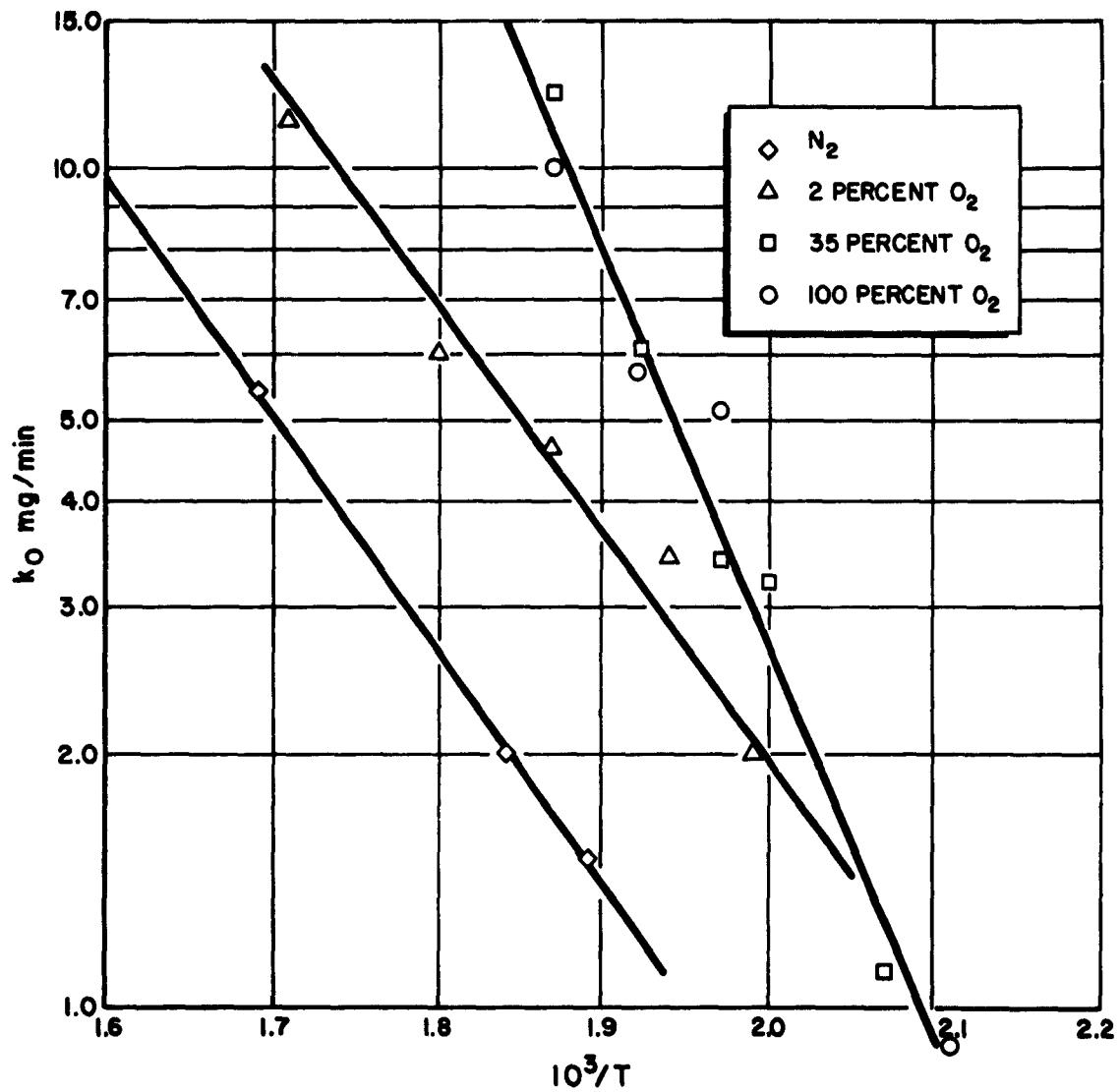


Figure 7. Zero-Order Rate Constants for PMMA Pyrolysis

**REFERENCES**

1. Burke, S. P. and T. E. W. Schumann: "Diffusion Flames," Industrial Engineering Chemistry, 20, 998 (1928).
2. R-3446, Research in Hybrid Combustion, Summary Report, 1 December 1960 to 30 November 1961, Rocketdyne, a Division of North American Aviation, Inc., Canoga Park, California, 30 January 1962.
3. R-2267-6, Research in Hybrid Combustion, Quarterly Report for Period Ending 28 February 1962, Rocketdyne, a Division of North American Aviation, Inc., Canoga Park, California, 31 March 1962.
4. R-2267-7, Research in Hybrid Combustion, Quarterly Report for Period Ending 30 May 1962, Rocketdyne, a Division of North American Aviation, Inc., Canoga Park, California, 30 June 1962.
5. R-2267-8, Research in Hybrid Combustion, Quarterly Report for Period Ending 31 August 1962, Rocketdyne, a Division of North American Aviation, Inc., Canoga Park, California, 16 January 1963.
6. Madorsky, S. L.: "Rates and Activation Energies of Thermal Degradation of Styrene and Acrylate Polymers in a Vacuum," J. Pol. Sci., VII, 491-506, 1953.
7. UTC 2007-QT2, Investigation of Fundamental Phenomena in Hybrid Propulsion, United Technology Corp., Sunnyvale, California, period ending 30 November 1961. CONFIDENTIAL.
8. LPC 594-S-1, Grain Design for Hybrid Motors, Lockheed Propulsion Co., Redlands, California, 22 January 1963. CONFIDENTIAL.